FEBS Letters 393 (1996) 226–230 FEBS 17494

Small-angle X-ray scattering reveals differences between the quaternary structures of oxygenated and deoxygenated tarantula hemocyanin

Heinz Decker[a,*], Hermann Hartmann[a], Reinhard Sterner[b], Erika Schwarz[c], Ingrid Pilz[c]

[a]*Institute of Molecular Biophysics, University of Mainz, Welder-Weg 26, D-55099 Mainz, Germany*
[b]*Department of Biophysical Chemistry, Biozentrum, University of Basel, Klingelbergstr. 70, CH-4056 Basel, Switzerland*
[c]*Institute for Physical Chemistry, University of Graz, Heinrichstr. 28, A-8010 Graz, Austria*

Received 24 June 1996; revised version received 30 July 1996

Abstract **Small-angle X-ray scattering (SAXS) curves have been recorded for the oxygenated and deoxygenated states of the 4×6-meric hemocyanin from the tarantula *Eurypelma californicum*. A comparison of the curves shows that the quaternary structures of the two states are different by three criteria, which all indicate that the hemocyanin is less compact in the oxygenated compared to the deoxygenated form: (a) The radius of gyration is 8.65 ± 0.05 nm for the deoxy- and 8.80 ± 0.05 nm for the oxy-form. (b) The maximum particle dimension amounts to 25.0 ± 0.5 nm for the deoxy- and to 27.0 ± 0.5 nm for the oxy-form. (c) A dip in the intramolecular distance distribution function *p(r)* is more pronounced and shifted to larger distances in the oxy-form. The *p(r)* functions based on SAXS measurements were compared to *p(r)* functions deduced from published electron microscopical images of three different 4×6-meric hemocyanins from closely related species. The *p(r)* functions of SAXS and electron microscopy were similar in one case, whereas in the other two cases the distance between the two 12-meric half-molecules had to be changed by 1–1.5 nm to obtain good agreement. The differences between the *p(r)* functions of oxygenated and deoxygenated 4×6-meric tarantula hemocyanin are much larger than one would expect from a comparison of X-ray structures of the oxygenated and deoxygenated states of a closely related 6-meric hemocyanin. Thus, the conformational changes upon oxygenation occur at various levels of the quaternary structure, as postulated by hierarchical theories of allosteric interactions.**

1. Introduction

Hemocyanins are extracellular multi-subunit oxygen carriers in the hemolymph of arthropods and molluscs [1–3]. They are of the size of ribosomes and small viruses with molecular masses ranging between $4.5 \cdot 10^5$ and $9.0 \cdot 10^6$ Da. For explaining the observed highly cooperative and allosteric oxygen binding behaviour, the existence of different conformations is postulated as well as transitions between them upon oxygenation. Small-angle X-ray scattering (SAXS) is the suitable method to detect conformational changes of large proteins in solution. This low-resolution technique has been applied successfully to monitor changes of the quaternary structure of a number of allosteric proteins such as hemoglobin [4], aspartate transcarbamoylase [5–8] glyceraldehyde-3-phosphate dehydrogenase [9], pyruvate kinase [10] and phosphofructokinase [11].

One of the best known hemocyanins is that from the tarantula *Eurypelma californicum* with a molecular mass of $1.8 \cdot 10^6$ Da. This 24-meric hemocyanin is composed of seven different subunit types, designated as *a* to *g* (Fig. 1). On the bases of electron microscopical images [12–14] the subunits are arranged in four hexamers. Each hexamer is composed of six non-identical subunits, containing types *a*, *d*, *e*, *f*, *g* and either *b* or *c*. As a consequence, there are two *b*- and two *c*-hexamers in the 24-mer. One *b*- and one *c*-hexamer are tightly connected and form a dodecamer (2×6-mer), representing the smallest structural repeating unit within the native 24-mer. Isologous dimerization of two dodecamers leads to the native molecule [12,15]. Oxygen binding of the tarantula hemocyanin is highly cooperative with Hill-coefficients of up to 9 [16], and both affinity and cooperativity of oxygen binding are sensitive to allosteric effectors such as protons [16,17]. To understand these functional properties, we have studied the quaternary structure changes that occur upon oxygen binding through SAXS measurements performed with the oxygenated and deoxygenated molecule. Our results show that the hemocyanin becomes less compact upon oxygenation and that changes in the quaternary structure occur at different structural levels of the 4×6-meric molecule.

2. Materials and methods

2.1. Preparation of the hemocyanin

Eurypelma californicum hemolymph was obtained by heart puncture as described elsewhere [18]. All samples were immediately diluted 1:2 (v/v) with 0.2 M Tris-HCl (pH 8.0), 10 mM $CaCl_2$, 10 mM $MgCl_2$. The samples were subsequently centrifuged for 10 min to remove blood cells. The hemocyanin was purified by gel filtration (TSK-HW 55, MERCK; 0.1 M Tris-HCl (pH 8.0), 5 mM $CaCl_2$, 5 mM $MgCl_2$ at 4°C). The large front peak contained pure 4×6-meric hemocyanin as shown by 2-dimensional immuno-gelelectrophoresis. Purified hemocyanin investigated under oxygenating conditions was dialysed against 0.1 M Tris-HCl, containing physiological concentrations of divalent cations (5 mM $CaCl_2$ and 5 mM $MgCl_2$, [19]). The pH value was adjusted to 8.5 at 4°C. Hemocyanin investigated under deoxygenating conditions was dialysed against the same buffer solution at pH 7.5. The hemocyanin was deoxygenated at 4°C with pure nitrogen in an atmos-bag (SIGMA) for 1 h as described previously [17].

Filling of the SAXS capillary with the deoxygenated hemocyanin was not possible within the atmos-bag. Instead, the hemocyanin was drawn up in the atmos-bag into a Pasteur pipette and immediately transferred to the capillary. The capillary was sealed within 10–20 s. The geometrical dimensions of both the Pasteur pipette and the capillary guarantee a very small surface/volume ratio of the hemocyanin solution, preventing reoxygenation of the hemocyanin during the filling procedure.

2.2. Small-angle X-ray scattering

Scattering experiments were performed using a Kratky camera with a slit collimation system. The X-ray generator (PHILIPS PW 1130) was operated at 50 kV and 30 mA, and sample solutions were exam-

*Corresponding author.

PII S0014-5793(96)00887-3

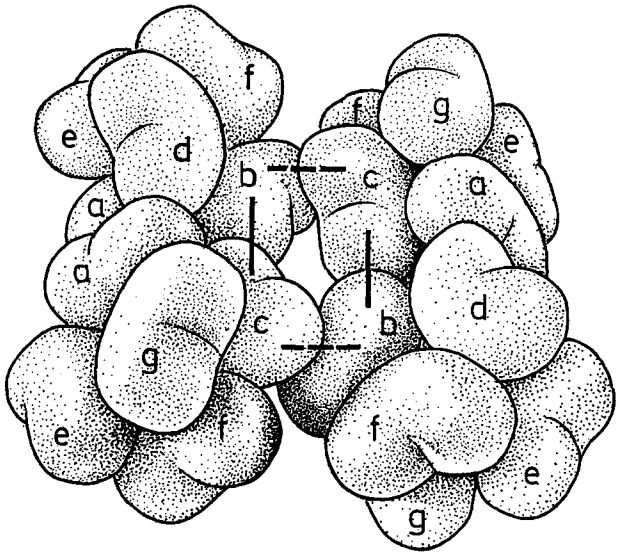

Fig. 1. Quaternary structure of 4×6-meric hemocyanin from the tarantula *Eurypelma californicum*. The tarantula hemocyanin is composed of 24 subunits, which belong to seven different types (designated with lower case letters *a* to *g* [12]). The subunits are arranged in four hexamers. Two hexamers, which contain either subunit *b* or *c*, form dodecamers that dimerize isologously to the native 24-meric hemocyanin (adapted from [29]).

ined at 4°C. Scattering curves were recorded several times at each concentration in order to minimize statistical errors. A single run lasted about 7 h. No radiation damage during the measuring procedure was detected when the scattering curves were plotted after different times of exposure to irradiation (data not shown).

Scattering intensities were recorded at 113 different angles, from $h = 0.1$ nm^{-1} to 4.08 nm^{-1} ($h = (4\pi/\lambda) \sin\theta$, 2θ = scattering angle, wavelength $\lambda = 0.154$ nm). About 120000 pulses were counted per point. Data evaluation, including smoothing, desmearing and indirect Fourier transformation were carried out with the computer program ITP. Details of the experimental technique and the evaluation procedure are described elsewhere [20,21]. Intraparticle distance distribution functions *p(r)* were calculated from the scattering curves *I(h)* using an indirect Fourier transformation according to Glatter [20,22].

In order to detect the largest possible structural differences, we investigated and compared only the fully oxygenated and the fully deoxygenated state. Different pH values were used for oxygenated and deoxygenated hemocyanin, respectively. As a result of the large Bohr effect of *Eurypelma* hemocyanin [16,17], oxygenation of the protein is promoted at the high pH value of 8.5, whereas the deoxy-state is stabilized at the lower pH value of 7.5. For the oxygenated form of the hemocyanin, two series of measurements were performed using five different concentrations, ranging from 7 to 39 g/l. For the deoxygenated hemocyanin, eight different concentrations were used ranging from 6 to 44 g/l.

2.3. *Calculation of* p(r) *functions from analyses of X-ray structures and electron microscopical images*

Atomic models of 4×6-meric hemocyanins were constructed on the basis of known X-ray structures of the homohexameric hemocyanin from *Limulus polyphemus* [23,24] composed of subunit II. The detailed parameter sets for the arrangement of the four hexamers were taken in form of relative translations and rotations from published analyses of electron microscopical images of native 4×6-meric hemocyanins from *Eurypelma californicum* [13] and *Androctonus australis* [25], as well as from the 4×6-meric dissociation product (half-molecule) of native 8×6-meric *Limulus polyphemus* hemocyanin [14]. From these models *p(r)* functions were calculated using all atomic coordinates.

The crystallographic X-ray coordinates of the oxy- and deoxy-hexamer of *Limulus* hemocyanin were obtained from the Brookhaven Protein Data Bank (PDB), entries 1OXY and 1LLA, respectively.

3. Results and discussion

3.1. *Radius of gyration and intraparticle distance distribution function* p(r)

The inner parts of the scattering curves were plotted according to Guinier [26] and extrapolated to zero concentrations. This plot gives a straight line with a slope proportional to the square of the radius of gyration (data not shown). After desmearing [22], radii of gyration (R_G) of 8.65 ± 0.05 nm and 8.80 ± 0.05 nm were obtained for the deoxy-hemocyanin and for the oxy-hemocyanin, respectively. The results indicate that tarantula hemocyanin becomes less compact upon oxygenation.

This view is in agreement with the experimentally obtained distance distribution functions *p(r)*. Here, the relative frequency of the distances between two scattering centers is plotted against the length of these distances. Fig. 2 shows *p(r)* functions for oxygenated and deoxygenated tarantula hemocyanin after extrapolation to zero concentration. The function *p(r)* drops to zero at values for *r* exceeding the maximum intraparticle distance D_{max}. According to this criterion, we obtained values for D_{max} of 27.0 ± 0.5 nm for the oxygenated hemocyanin, being significantly larger than the value 25.0 ± 0.5 nm for the deoxygenated hemocyanin. From these *p(r)* functions values of 8.81 nm and 8.65 nm were calculated for R_G, respectively. They agree well with the values obtained independently from the Guinier-plot as mentioned above. In addition, the oxy-state is different from the deoxy-state when the shapes of the *p(r)* functions are compared (Fig. 2). The dip at the maximum indicates that compact masses are separated by a cleft with less mass density [20]. In the oxy-state the dip is more pronounced and shifted to longer distances, indicating that the arrangement of the four 6-mers is less compact compared with the deoxy-state.

3.2. *Comparison of* p(r) *functions as obtained by SAXS and by electron microscopy*

We compared the *p(r)* functions of 4×6-meric tarantula hemocyanin obtained by SAXS with *p(r)* functions that

Table 1
Values for the radius of gyration R_G and the maximum particle distance D_{max} for 24-meric hemocyanins from closely related chelicerata, the tarantula *Eurypelma californicum*, the scorpion *Androctonus australis*, and the horseshoe crab *Limulus polyphemus*

Species	R_G [nm]	$d_{12mer-12mer}$ [nm]	Notes	Reference
E. californicum oxy-form	8.80 ± 0.05	-	SAXS	this study
E. californicum deoxy-form	8.65 ± 0.05	-	SAXS	this study
E. californicum	9.24	11.9	EM, n.s.	[13]
E. californicum	8.80	10.5	corrected	this study
L. polyphemus	8.78[a]	10.8	EM, n.s.	[14]
L. polyphemus	9.13[a] ± 0.14	-	SAXS[b]	[31]
A. australis	9.22	11.6	EM, i.e.	[25]
A. australis	8.85	10.5	corrected	this study

The values were obtained experimentally from small angle X-ray scattering experiments (SAXS) or from reconstructed 4×6-mers based on the analyses of electron microscopical images (EM), which were either negatively stained (n.s.) or ice embedded (i.e.).
[a]The reason for the discrepancy betweeen these R_G values is not clear.
[b]This value was obtained for the 4×6-meric intermediate after dissociation of the 8×6-meric hemocyanin.

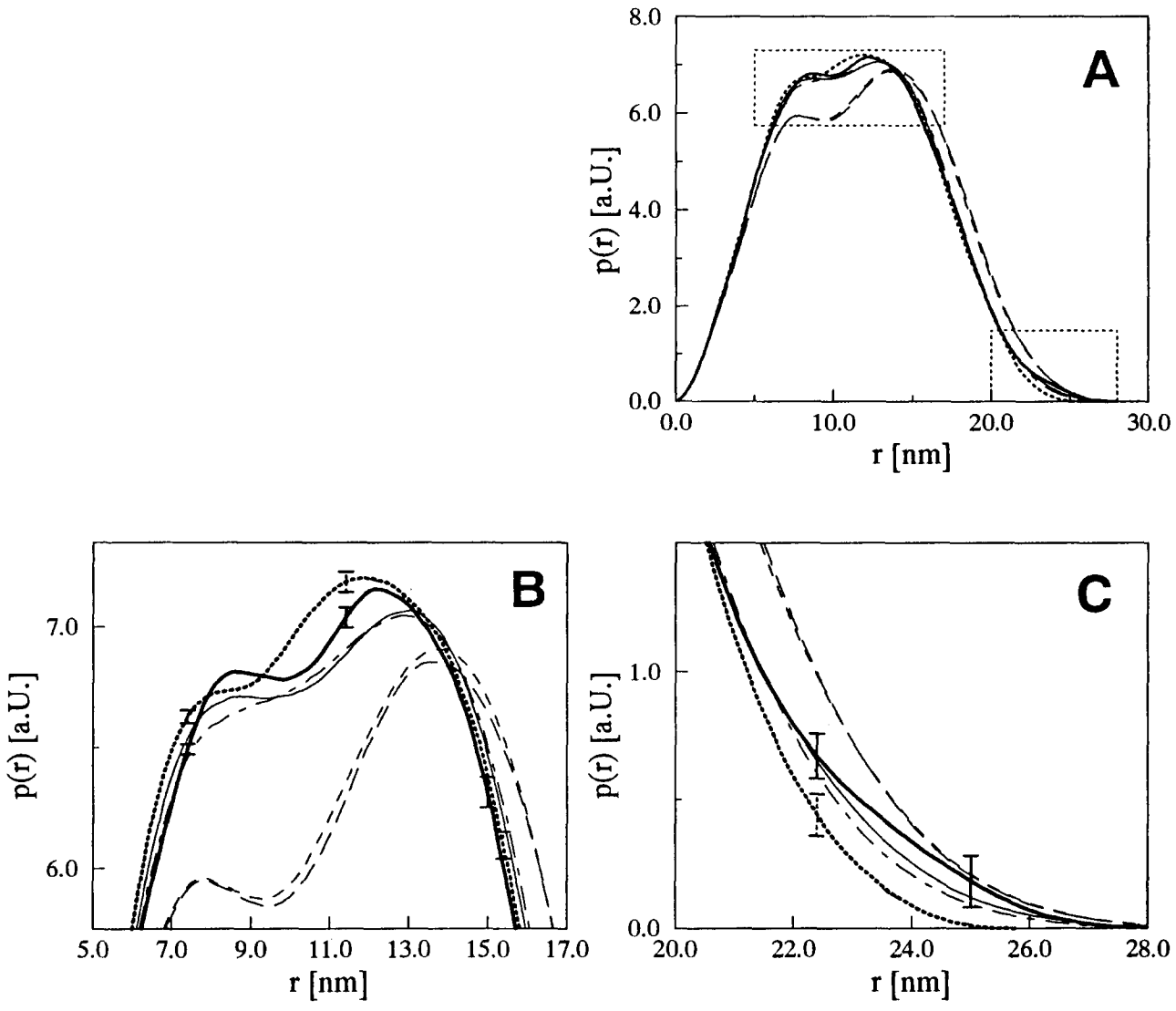

Fig. 2. Comparison of $p(r)$ functions of 4×6-meric hemocyanins as obtained by SAXS and electron microscopy. $P(r)$ functions are shown completely (A), and enlarged near their maxima (B) or at large distances (C). Symbols: oxygenated (———) and deoxygenated (• • •) hemocyanin from *E. californicum* as obtained by SAXS; hemocyanin from *E. californicum* (– – –) [13], *A. australis* (- - -) [25] and *L. polyphemus* (———) [14] as deduced from electron microscopical image analyses; (– • –) hemocyanin from *E. californicum* as obtained by electron microscopy after correction of the distance between the two dodecameric half-molecules from 11.9 nm to 10.5 nm.

were deduced from electron microscopical images of the tarantula hemocyanin itself [13], the 4×6-meric hemocyanin from *Androctonus australis* [25], and the 4×6-meric half-molecule of 8×6-meric hemocyanin from *Limulus polyphemus* [14] (Fig. 2).

Comparing the three models from electron microscopical images, the best agreement with our SAXS data is obtained with 4×6-meric *Limulus* hemocyanin. In contrast, electron microscopy based $p(r)$ functions of *Eurypelma* and *Androctonus* hemocyanin show obvious deviations from the distance distributions as determined by SAXS. A better agreement between electron microscopy and SAXS data is obtained when the distance between the axes along the dodecamers is shortened from about 11.9 nm, as determined by electron microscopy [13,25] to 10.5 nm (Fig. 3). It should be pointed out that the distance of 11.9 nm was determined from analyses of electron microscopical images, no matter whether they were negatively stained, as in the case of *Eurypelma* hemocyanin, or ice embedded, as in the case of *Androctonus* hemocyanin. In accordance with our corrected inter-dodecamer distance for *Eurypelma* and *Androctonus* hemocyanin, a value of 10.8 ± 0.5 nm was found for the 4×6-meric *Limulus* hemocyanin based on negatively stained electron microscopical images [14]. We calculated R_G values of 8.78 nm, 8.80 nm and 8.85 nm for the 4×6-meric *Limulus* hemocyanin and the corrected models of *Eurypelma* and *Androctonus* hemocyanin, respectively. They are in a good agreement with the value of 8.80 ± 0.05 nm, which was obtained experimentally by our SAXS measurements with the oxy-form (Table 1). In addition, the shapes of the $p(r)$ functions calculated from these corrected models are similar to those of the oxy-form (Fig. 2).

3.3. *At which level of the quaternary structure do differences occur between the oxygenated and the deoxygenated 4×6-meric tarantula hemocyanin?*

To answer this question, the highly resolved X-ray struc-

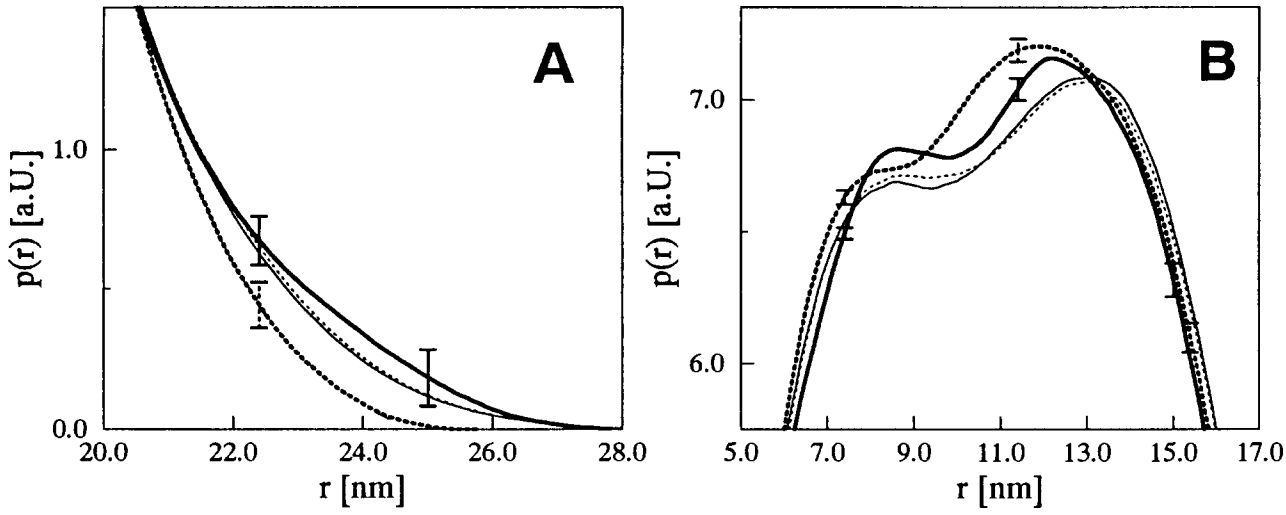

Fig. 3. Conformational changes upon oxygen binding to 4×6-meric tarantula hemocyanin occur at different levels of the quaternary structure. Enlarged *p(r)* functions are shown at large distances (A) and near their maxima (B). The *p(r)* functions of the 4×6-meric tarantula hemocyanin in its oxygenated (———) and its deoxygenated (• • •) state were obtained from SAXS experiments. *P(r)* functions for 4×6-meric *L. polyphemus* hemocyanin were calculated from published data as follows: X-ray structures of the oxygenated and the deoxygenated 1×6-mer [23,24] were arranged in the same way to 'oxygenated' (———) and 'deoxygenated' (·····) 4×6-mers according to electron microscopical images [14], i.e. no differences between the oxy- and deoxy-states were assumed with respect to the arrangement of the four hexamers. Since the differences in the *p(r)* functions between the 'oxygenated' and the 'deoxygenated' 4×6-meric *L. polyphemus* hemocyanin are negligible compared to those between the oxygenated and the deoxygenated 4×6-meric tarantula hemocyanin, changes in the quaternary structure at a level higher than that of 6-mers must occur upon oxygen binding.

tures of oxygenated and deoxygenated homohexameric hemocyanins from *Limulus polyphemus* [23,24] were assembled to 4×6-mers, using electron microscopical images as described above. In this approach, the arrangement of the four hexamers is identical in the oxy- and deoxy-state. Thus, changes in the structure are restricted artificially to the level of the 6-mers, which show only a weak cooperativity of oxygen binding [27] and where significant differences between the oxy- and the deoxy-forms could be detected only at the active site [23,24]. The 4×6-meric dissociation intermediate of the native 8×6-mer, however, binds oxygen with high cooperativity [28]. Fig. 3 shows that the resulting *p(r)* functions of the reconstructed *Limulus* 4×-homohexamer are very similar for the oxy- and deoxy-states. In contrast, the measured oxy- and deoxygenated states of native 4×6-meric tarantula hemocyanin show considerable differences (Figs. 2 and 3). This result suggests that major changes in the quaternary structure must also occur at levels higher than the 6-mer. This idea is supported by the fact that the dip in the *p(r)* function is more pronounced and shifted to longer distances in the oxy-state (Figs. 2 and 3), indicating that the four hexamers move apart from each other upon oxygen binding. In accordance with these findings, Savel-Niemann et al. [29] showed that the full cooperativity of oxygen binding of tarantula hemocyanin is drastically decreased at the level of the 1×6-mer and 2×6-mer, compared to the native 4×6-mer. Thus, our results suggest that conformational changes upon oxygen binding occur at various levels of the quaternary structure. This finding is consistent with hierarchical theories of allosteric interactions such as the recently developed Nesting model [30].

Acknowledgements: Ingrid Pilz and Erika Schwarz thank the Österreichischen Fond zur Förderung der wissenschaftlichen Forschung for generous support. Heinz Decker was supported by the Deutsche Forschungsgemeinschaft (Grant De 414/4-1).

We thank Dr. Kasper Kirschner for helpful discussions, and Dr. Christine Wright and Bernhard Lohkamp for critical reading of the manuscript.

References

[1] Van Holde, K.E. and Miller, K.I. (1995) Adv. Protein Chem. 47, 1–74.
[2] Ellerton, H.D., Ellerton, N.F. and Robinson, H.A. (1983) Proc. Biophys. Mol. Biol. 41, 143–248.
[3] Markl, J. and Decker H. (1992) Adv. Comp. Environ. Physiol. 13, 325–376.
[4] Conrad, H., Mayer, A., Thomas, H.P. and Vogel, H. (1969) J. Mol. Biol. 41, 225–229.
[5] Moody, M.F., Vachette, P. and Foote, A.M. (1979) J. Mol. Biol. 133, 517–532.
[6] Herve, G., Moody, M.F., Tauc, P., Vachette, P. and Jones, P.T. (1985) J. Mol. Biol. 185, 189–199.
[7] Kihara, H., Takahashi-Ushijima, E., Amemiya, Y., Honda, Y., Vachette, P., Tauc, P., Barman, T.E., Jones, P.T. and Moody, M.F. (1987) J. Mol. Biol. 198, 745–748.
[8] Tauc, P., Vachette, P., Middleton, S.A. and Kantrowitz, E.R. (1990) J. Mol. Biol. 214, 327–335.
[9] Durchschlag, H., Puchwein, G., Kratky, O., Schuster, I. and Kirschner, K. (1971) Eur. J. Biochem. 19, 9–22.
[10] Müller, K., Kratky, O., Rischlau, P. and Hess, B. (1972) Hoppe-Seyler's Z Physiol. Chem. 353, 803–809.
[11] Paradies, H.H. and Vettermann, W. (1978) Arch. Biochem. Biophys. 191, 169–181.
[12] Markl, J., Kempter, B., Linzen, B., Bijlholt, M.M.C. and van Bruggen, E.F.J. (1981) Hoppe-Seyler's Z Physiol. Chem. 362, 1631–1641.
[13] De Haas, F. and van Bruggen, E.F.J. (1994) J. Mol. Biol. 237, 464–478.
[14] Van Heel, M. and Dube, P. (1994) Micron 25, 387–418.
[15] Markl, J., Decker, H., Linzen, B., Schutter, W.G. and van Bruggen, E.F.J. (1982) Hoppe-Seyler's Z Physiol. Chem. 363, 73–87.
[16] Loewe, R. (1978) J. Comp. Physiol. B 128, 161–168.
[17] Decker, H. and Sterner, R. (1990) J. Mol. Biol. 211, 281–293.
[18] Markl, J., Strych, W., Schartau, W., Schneider, H.-J., Schöberl, P. and Linzen, B. (1979) Hoppe-Seyler's Z Physiol. Chem. 360, 639–650.

[19] Schartau, W. and Leidescher, T. (1983) J. Comp. Physiol. 152, 73–77.
[20] Glatter, O. and Kratky, O. (1982) Small Angle X-Ray Scattering, Academic Press, London.
[21] Pilz, I., Glatter, O. and Kratky, O. (1979) Methods Enzymol. 61, 148–249.
[22] Glatter, O. (1980) Acta Phys. Austrica 52, 243–256.
[23] Magnus, K.A., Hazes, B., Ton-That, H., Bonaventura, C., Bonaventura, J. and Hol, W.G.J. (1994) Proteins: Struct. Funct. Genet. 19, 302–309.
[24] Hazes, B., Magnus, K.A., Bonaventura, C., Bonaventura, J., Dauter, Z., Kalk, K.H. and Hol, W.G.J. (1993) Protein Sci. 2, 597–619.
[25] Boisset, N.P., Penczek, J.-C., Taveau, J., Lamy, J., Frank, J. and Lamy, J. (1995) J. Struct. Biol. 115, 16–29.
[26] Guinier, A. (1963) X-ray Diffraction in Crystals, Imperfect Crystals, and Amorphous Bodies. (W.H. Freeman and Company, San Francisco, CA).
[27] Brenowitz, M., Bonaventura, C. and Bonaventura, J. (1984) Arch. Biochem. Biophys. 230, 238–249.
[28] Brouwer, M. and Serigstad, B. (1989) Biochemistry 28, 8819–8827.
[29] Savel-Niemann, A., Markl, J. and Linzen, B. (1988) J. Mol. Biol. 204, 385–395.
[30] Robert, C.H., Decker, H., Richey, B., Gill, S.J and Wyman, J. (1987) Proc. Natl. Acad. Sci. USA 84, 1891–1895.
[31] Kimura, K., Igarashi, Y., Kajita, A., Wang, Z.-X., Tsuruta, H., Amemiya, Y. and Kihara, H. (1990) Biophys. Chem. 38, 23–32.